



Southeast Environmental Research Center
FLORIDA INTERNATIONAL UNIVERSITY

Mapping and Assessing Fire Damage on Broadleaved Forest Communities in Big Cypress National Preserve



Pablo L. Ruiz¹
Jay P. Sah¹
James R. Snyder³
Michael S. Ross^{1,2}

September 11, 2012

USGS Cooperative Agreement # G11AC20030

¹Southeast Environmental Research Center, Florida International University, Miami, FL 33199

²Department of Earth and Environment, Florida International University, Miami, FL 33199

³U.S. Geological Survey, Southeast Ecological Science Center, Ochopee, FL 34141

Table of Contents

1. Introduction	1
2. Method	2
2.1 Study Area	2
2.2 Vegetation mapping	3
2.3 Accuracy assessment	4
2.4 Burn severity	5
3. Results	6
3.1 Vegetation map	6
3.2 Burn severity	7
4. Discussion	8
 References	 10

List of Tables

	Page
Table 1: List of community types mapped using airborne imagery with descriptions and the total number of patches (polygons) and their combined area.	3
Table 2: Spectral indices used to enhance the spectral resolution of the 2009 natural color orthophotos.	4
Table 3: Ordinal burn severity levels and dNBR ranges (scaled by 10^3).	5
Table 4: Error matrix for the thematic mapped produced.	7

List of Figures

Figure 1: Site map showing the location of the Deep Fire within Big Cypress National Preserve.	2
Figure 2: Thematic map of oak-dominated forest and hammocks within the Deep Fire.	11
Figure 3: Burn severity (dNBR) map of oak-dominated forests and hammocks Within the Deep Fire.	12
Figure 4: Pre- and post-fire differences in (a) RGB-Reflectance, and (b) $G_{NDVI}PVI$ For the oak-dominated forest and hammocks within the Deep Fire (2009)	13
Figure 5: Correlation between dNBR and (a) ΔRGB -Reflectance(%) and (b) $\Delta G_{NDVI}PVI$ (%)	14

1. Introduction

Within Big Cypress National Preserve (BICY), oak-dominated forests and woodlands as well as tropical and temperate hardwood hammocks are integral components of the landscape and are biodiversity hotspots for both flora and fauna. These broadleaved forest communities serve as refugia for many of the Preserve's wildlife species during prolonged flooding and fires. However, both prolonged flooding and severe fires, which are important and necessary disturbance vectors within this landscape, can have deleterious effects on these forested communities. This is particularly true in the case of fires, which under extreme conditions associated with drought and elevated fuel loads, can burn through these forested communities consuming litter and understory vegetation and top killing most, if not all, of the trees present.

In South Florida, lightning fires, which usually occur in the wet season as a result of thunderstorms, tend to be generally small and rarely severe (Wade et al. 1980; Snyder 1991). However, fires at the start of the rainy season under drought conditions can spread quickly through the landscape and burn for several weeks, consuming thousands of hectares (ha) before being controlled and suppressed. These early season fires are typically associated with high ambient temperatures and low humidity (Slocum et al. 2007), and thus tend to burn relatively hot and pose the greatest risk to all biological resources within BICY. One such fire, the Deep Fire, burned 12,000 ha within BICY between April 22 and May 11, 2009, and caused widespread canopy damage, including tree mortality, on many of the oak-dominated forests and hammock communities present within the Deep Fire incident boundary (**Figure 1**). Another source of fire within this landscape is anthropogenic fires. These fires, which typically occur in winter and early spring, tend to be relatively small in size and just like early season lightning fires can burn extremely hot and cause severe damage to these forested communities.

Due to the high incidence of both natural and anthropogenic fires within BICY, it is important for ecologists and resource managers working within BICY to 1) document and understand how fire interacts with these forested communities, and 2) understand how biodiversity and successional processes within these forested communities are affected by fire. Among the first steps in accomplishing these tasks is to have a spatially and thematically accurate map of these forested communities and a geodatabase that includes information regarding their structure and composition as well as their fire history. This information would then be used to document and monitor fire effects and post-fire recovery and succession over time.

With a major goal of understating the role of fire in shaping the landscape within BICY, the primary objective of our research was to quantify the effects of the Deep Fire on the broadleaved forest communities present within the fire incident boundary (**Figure 1**). Our approach was twofold: first, we developed a pre-fire base map of all oak-dominated communities and hammocks within the Deep Fire boundary using airborne imagery taken three months prior to the fire, and then assessed broad-scale fire effects within these communities through the use of spectral indices (SI) derived from Landsat TM multispectral resolution imagery acquired three months pre-fire (Jan 2009) and eight months post-fire (Jan 2010).

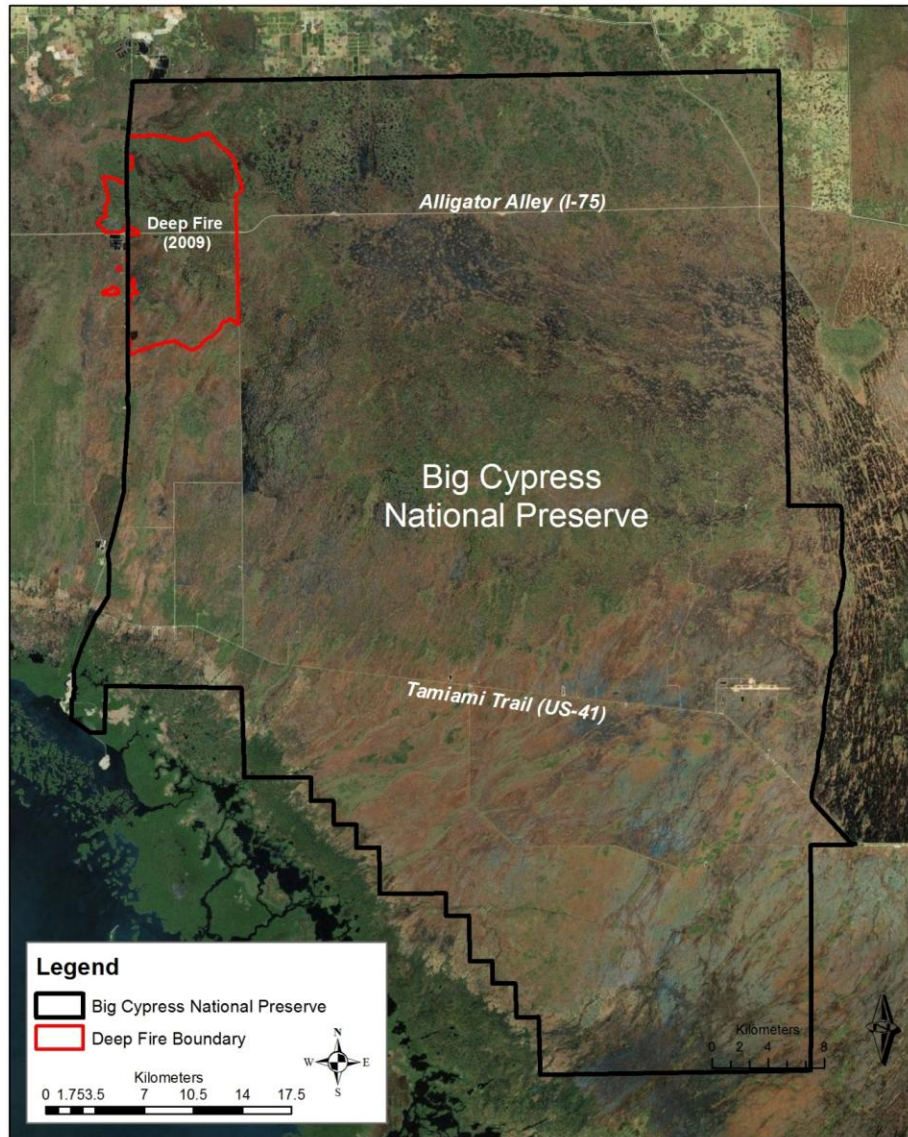


Figure 1: Site map showing the location of the Deep Fire within Big Cypress National Preserve

2. Methods

2.1 Study Area

This study was conducted within the perimeter of the Deep Fire in Big Cypress National Preserve, Florida, USA (**Figure 1**). The Deep Fire, which burned for 20 days between April and May 2009, was a lightning-ignited fire resulting from the onset of the rainy season in southwest Florida. Aerial surveys during the fire suppression phase and immediately thereafter, indicated that many of the oak-dominated forests and woodlands present within the fire boundary had been significantly damaged with large numbers of oaks and other hardwood tree species having been topkilled.

2.2 Vegetation Mapping

All oak-dominated forest and woodlands as well as broadleaved hammocks $\geq 400 \text{ m}^2$ within the Deep Fire boundary were identified, screen-digitized, and populated into an ESRI® ArcMap TM 9.3 geodatabase. The basemap used to create the vegetation map was derived from 60-cm spatial resolution natural color (Red, Green, Blue) compressed (30:1) Mosaic/MS3 orthophotos acquired in January 2009 by SURDEX Corporation. However, because of the spatial complexity of the landscape, the spectral similarity associated with the communities being mapped, and the compression algorithm (i.e., Mosaic/MS3) used by SURDEX Corporation, the natural color orthophotos proved to be inadequate for discriminating among target communities (**Table 1**). Consequently, we enhanced the spectral resolution of the original orthophotos, by calculating six spectral indices (**Table 2**) derived from the three original orthophoto spectral bands (Red, Green, Blue). These six spectral indices were then stacked, a process of combining multiple images or rasters into a single image, onto the original orthophotos. The resulting 9-band stacked mosaic image (Red, Green, Blue, Pan, GRPVI, PVR, PPR, SI01, SI02) was resampled to a 1-m spatial resolution to reduce image size and improve computer processing time.

Table 1: List of community types mapped using airborne imagery with descriptions and the total number of patches (polygons) and their combined area.

Community Type	Description	No. of Patches	Total Area (ha)
Mixed-Hardwood Hammock	Closed canopy (>60%) high density forests dominated by evergreen and semi-deciduous tropical and temperate broad-leaved trees. These forests tend to be more hydric than similarly structured Tropical Hardwood Hammocks.	59	175.6
Oak-Cabbage Palm Hammock	Closed canopy (>60%) high-density stands of a co-dominant mix (40-60%) of southern live oak (<i>Quercus virginiana</i>) and cabbage palm (<i>Sabal palmetto</i>).	157	1,187.9
Oak Hammock	Closed canopy (>60%) stands dominated by southern live oak (<i>Quercus virginiana</i>). Other canopy species may include cabbage palm (<i>Sabal palmetto</i>) as well as tropical and temperate broad-leaved trees.	58	144.3
Oak-Saw Palmetto Woodland	Open canopy (10-60%) stands of southern live oak (<i>Quercus virginiana</i>) dominated by saw palmetto (<i>Serenoa repens</i>) in the understory. Cabbage palm and other tree species maybe present	313	390.1
Tropical Hardwood Hammock	Closed canopy (>60%) high density forests dominated by broad-leaved evergreen and semi-deciduous tropical tree species.	10	10.0

Table 2: Spectral indices used to enhance the spectral resolution of the 2009 natural color orthophotos.

Band #	Index	Formula
4	Panchromatic (Pan)	(Red + Green + Blue) / 3
5	Green-Red Percentage Vegetation Index (GRPVI) ^a	Green / (Green + Red); increases with vegetation cover
6	Photosynthetic Vigor Ratio (PVR) ^b	Green / Red; high for strong chlorophyll absorption
7	Plant Pigment Ratio (PPR) ^b	Green / Blue; high for highly pigmented foliage
8	SI01	Green / (Red + Blue)
9	SI02	Green / (Red – Blue)

^aderived from Motohka et al. 2010; ^bWarren & Metternicht 2005.

Ocular examination of several 3-band combinations from the newly created 9-band stacked image revealed a marked improvement over the original natural color orthophotos when it came to distinguishing our targeted communities from other wooded communities (e.g., Pine Forest or Cypress Swamps). Furthermore, some band index combinations, e.g., GRPVI, SI02, Blue, were better suited than others, e.g., Red, GRPVI, Blue, at this task. As a result, using ERDAS Imagine 9.3, we performed a principal component analysis (PCA) on the 9-band stacked image to reduce the dimensionality of the data into fewer and easier-to-interpret uncorrelated variables or principal components (PC).

The first three PC explained 98% of the variance observed. When stacked into a new 3-band PC, the image significantly improved our ability to differentiate the target communities from other woody communities and the adjacent marsh. However, it proved impossible to systematically distinguish and classify the targeted communities using ISODATA clustering algorithm—an iterative process that groups spectrally similar pixels into clusters that are a posteriori classified into meaningful thematic classes. Nonetheless, the resulting 3-band PC stacked image allowed us to pinpoint the location of our targeted communities and to manually digitize and classify them into one of five structural and compositional categories: Mixed Hardwood Hammock, Oak Hammock, Oak-Cabbage Palm Hammock, Oak-Saw Palmetto Woodland, or Tropical Hardwood Hammock (**Table 1**).

2.3 Accuracy Assessment

One-hundred accuracy assessment points (AAP) were selected at random from all polygons mapped. AAPs were accessed by helicopter and classified using the categories outline in **Table 1**. However, because of flight time restrictions, the total area need to be covered, and the difficulty associated in classifying post-fire communities to their pre-fire conditions, we were only able to sample 36 of the intended 100 AAPs selected.

2.4 Burn Severity

Broad-scale post-fire burn severity within the mapped communities was assessed using multitemporal (pre- and post-fire) medium spatial resolution (30 m pixel) Landsat TM multispectral imagery. The two imagery were from Jan-2009, three months before fire, and Jan-2010, eight months after fire. The raw spectral data for each Landsat TM image was corrected to at satellite reflectance and atmospherically corrected in ENVI 5.0 to standardize each Landsat TM image and correct for atmospheric transmittance. The Landsat TM imagery were then resampled to a 1-meter spatial resolution to match the fine scale, 1:1,000 on screen resolution, used to map community boundaries and clipped to encompass only the area affected by the Deep Fire.

Following image standardization and resampling, we calculated the following spectral indices for each polygon mapped: NBR and dNBR as well as RGB-Reflectance and $G_{NDVI}PVI$. While NBR and dNBR have been used extensively to assess burn severity by the US Forest Service and others (e.g., Escuin et al. 2008), RGB-Reflectance and $G_{NDVI}PVI$ have never been used in this capacity and are introduced as potential surrogates to dNBR.

NBR and dNBR are defined as:

$$NBR = 1000 * (\rho(\lambda_{NIR}) - \rho(\lambda_{MIR})) / (\rho(\lambda_{NIR}) + \rho(\lambda_{MIR})) \quad (1)$$

$$dNBR = NBR_{pre-fire} - NBR_{post-fire} \quad (2)$$

where $\rho(\lambda_{NIR})$ and $\rho(\lambda_{MIR})$ represent spectral reflectance in the near-infrared and mid-infrared portions of the electromagnetic spectrum for each Landsat TM image, respectively, and dNBR is the difference between the pre- and post-fire NBR values. dNBR has a theoretical range between -2,000 to +2,000, when scaled by 10^3 , but values < -500 and $> +1,300$ are not typical and usually the result of image anomalies not related to temporal bio-physical differences in land cover resulting from fire (**Eq. 2**; Key and Benson 2006). Values $< +100$ generally represent unburned or enhanced regrowth following a fire while values $\geq +100$ indicate increasing burn severity (**Table 3**; Key and Benson 2006).

Table 3: Ordinal burn severity levels and dNBR ranges (scaled by 10^3).

Burn Severity Level	dNBR Range
Enhance Regrowth, High	-500 to -251
Enhance Regrowth, Low	-250 to -101
Unburned	-100 to +99
Low Severity	+100 to +269
Moderate/Low Severity	+270 to +439
Moderate/High Severity	+440 to +659
High Severity	+660 to +1300

RGB-Reflectance is defined as:

$$\text{RGB-Reflectance} = \rho(\lambda_{\text{red}}) + \rho(\lambda_{\text{green}}) + \rho(\lambda_{\text{blue}}) \quad (3)$$

where $\rho(\lambda_{\text{red}})$, $\rho(\lambda_{\text{green}})$, and $\rho(\lambda_{\text{blue}})$ represent spectral reflectance in the visible spectral portion of the electromagnetic spectrum. We expected to see an increase in the overall RGB-Reflectance between the pre- and post-fire Landsat TM images for the plant communities mapped. Furthermore, we expect that high RGB-Reflectance values in the 2010 Landsat TM imagery will be indicative of areas with high burn severity and should be positively correlated to dNBR; that is, as dNBR increases, RGB-Reflectance should also increase in response to a decrease in live biomass and absorption of blue and red wavelengths by palisade mesophyll (e.g., chlorophyll *a* and *b*, and β -carotene).

The Green-NDVI Percentage Vegetation Index ($G_{\text{NDVI}}\text{PVI}$) is a derivative of Green-NDVI (Gitelson et al. 1996) and is defined as:

$$G_{\text{NDVI}}\text{PVI} = \rho(\lambda_{\text{NIR}}) / (\rho(\lambda_{\text{NIR}}) + \rho(\lambda_{\text{green}})) \quad (4)$$

where $\rho(\lambda_{\text{NIR}})$ and $\rho(\lambda_{\text{green}})$ represent spectral reflectance in the near-infrared and green portions of the electromagnetic spectrum, respectively. The values for this index range from 0 to +1 and increase as a function of increasing vegetation cover and photosynthetic vigor. As a result, we expect to see an overall decrease in the $G_{\text{NDVI}}\text{PVI}$ between pre- and post-fire Landsat TM images for those plant communities mapped that burned during the fire, particularly in areas where the fire was most severe. Furthermore, we expect that low $G_{\text{NDVI}}\text{PVI}$ values in the 2010 Landsat TM imagery will be indicative of fire damage and should be negatively correlated to dNBR; that is, as dNBR increases, indicating high burn severity, the $G_{\text{NDVI}}\text{PVI}$ values should decrease to reflect a decrease in live biomass and reflectance in the green wavelength.

Lastly, a zonal mean function was used to calculate the mean pre- and post-fire RGB-Reflectance, $G_{\text{NDVI}}\text{PVI}$ and dNBR for each community mapped. Using the zonal mean of each community mapped, we calculated the pre- and post-fire percent change $\Delta(\%)$ in RGB-Reflectance and $G_{\text{NDVI}}\text{PVI}$ for each polygon mapped as followed:

$$\Delta(\%) = ((t_2 - t_1) / t_1) * 100 \quad (5)$$

where t_1 and t_2 represent the pre- and post-fire zonal mean spectral index values, respectively, for each polygon. Between-year difference in RGB-Reflectance and $G_{\text{NDVI}}\text{PVI}$ were tested using Student's *t*-test. Univariate regression analysis was then used to relate $\Delta\text{RGB-Reflectance}(\%)$ and $\Delta G_{\text{NDVI}}\text{PVI}(\%)$ between 2009 and 2010 to dNBR. All statistical analyses were done in Statistica 7.0 (StatSoft Inc. 2005).

3. Results

3.1 Vegetation Map

The vegetation map produced contains a total of 597 forested patches encompassing 1,908 ha (**Figure 2**). The most numerous community type mapped within the fire boundary was Oak-Saw Palmetto Woodland with 313 patches (**Table 1**). However, Oak-Cabbage Palm Hammocks had the greatest overall coverage with nearly 1,200 ha mapped and an average patch size of approximately 7.5 ha. Tropical Hardwood Hammocks, on the other hand, were the least common community types found and mapped with only ten patches encompassing no more than 10 ha in total.

Overall map accuracy was 78% with a K_{hat} statistic (i.e., a measure of accuracy between the thematic map and the reference data) of 70%. Producer accuracy (i.e., the percentage of a given class that is correctly identified on the map) was very good for Mixed Hardwood Hammock, Oak Hammocks, and Oak-Cabbage Palm Hammock, but poor for Oak-Saw Palmetto Woodland and Tropical Hardwood Hammock (**Table 4**). In contrast, the user's accuracy (i.e., the probability that a given pixel will appear on the ground as it is classed) was very low, < 80%, for Mixed Hardwood Hammock, Oak Hammocks, and Oak-Cabbage Palm Hammock but high, 100%, for Oak-Saw Palmetto Woodland and Tropical Hardwood Hammock (**Table 4**).

Table 4: Error matrix for the thematic mapped produced.

Mapped	Observed					Row Total	User's Accuracy (%)
	Mixed Hardwood Hammock	Oak Hammock	Oak-Cabbage Palm Hammock	Oak-Saw Palmetto Woodland	Tropical Hardwood Hammock		
Mixed Hardwood Hammock	2		1	2		5	40
Oak Hammock		7		1	1	9	78
Oak-Cabbage Palm Hammock			5	2	1	8	63
Oak-Saw Palmetto Woodland				12		12	100
Tropical Hardwood Hammock					2	2	100
Column Total	2	7	6	17	4	36	0.78
Producer's Accuracy (%)	100	100	83	71	50	$K_{\text{hat}} = 0.70$	

3.2 Burn Severity

Post-fire assessment of burn severity, through dNBR, revealed a patch-mosaic of fire damage and recovery for the oak-dominated communities and hammocks within the Deep Fire (**Figure 3**). Even eight months after the fire, 43.5% of these communities still showed evidence of low to

moderate burn severity, while 56.1% showed no signs of having burned. Enhanced regrowth was observed in some areas but accounted for only 0.4% (**Figure 3**).

As expected, the RGB-Reflectance for the communities mapped increased while $G_{NDVI}PVI$ decreased following the fire (**Figure 4**). Pre- and post-fire differences in community RGB-Reflectance and $G_{NDVI}PVI$ were significant ($t_{(594)} = -29.2$ and 35.8 , respectively; $P < 0.001$). On average, RGB-Reflectance values were 0.017 higher while $G_{NDVI}PVI$ values were 3.3% lower eight months following the fire (**Figure 4**).

Percent change in both the RGB-Reflectance and $G_{NDVI}PVI$ indices were significantly correlated ($P < 0.001$) to dNBR and increasing burn severity (**Figure 5**). As expected, $\Delta RGB\text{-Reflectance}(\%)$ was positively correlated to dNBR while $\Delta G_{NDVI}PVI(\%)$ was negatively correlated (**Figure 5**). However, $\Delta G_{NDVI}PVI(\%)$ showed a stronger correlation with dNBR than did $\Delta RGB\text{-Reflectance}(\%)$ ($r = -0.862$ vs $r = 0.390$, respectively).

4. Discussion:

The accuracy of the map produced, 78%, and k_{hat} statistic, 70%, was good but not within the standard of $>80\%$ set by the USGS/NPS Vegetation Mapping Program protocols (TNC and ESRI 1994). Yet, for individual thematic classes the producer's and user's accuracy of $>80\%$ was met (**Table 4**). The low number of AAPs sampled (36 out of the intended 100) and the post-fire determination of pre-fire communities during the accuracy assessment phase very likely contributed to the lower than expected map accuracy and low K_{hat} statistic. Furthermore, the accuracy of the thematic classes was limited by the spatial and spectral resolution of the imagery and its delivered format (i.e., MRSID/MG3), which impeded our ability to accurately identify and map the targeted communities. Nonetheless, when compared to previous mapping efforts for the same area within BICY (see Welch et al. 1999), we find that this map did a much better job at identifying and mapping the oak-dominated forest and woodlands as well as tropical and temperate hardwood hammocks within the Deep Fire boundary. Consequently, as a management, monitoring, and inventory tool, this map of the Deep Fire should help managers and researchers identify the locations of these communities within the Deep Fire and to monitor their post-fire recovery and successional processes.

The dNBR burn severity map made eight months after the fire (**Figure 3**) indicates that the majority of the communities burned during the Deep Fire were well into recovery by then. Burn severity for the mapped communities ranged between low and moderate/high burn severity, with few if any of the mapped communities experiencing high burn severity (**Figure 3**). This is somewhat surprising considering the intensity of the fire and the ground based observations made during fire suppression (see Watts et al. 2012). However, in southern neo-tropical peninsular Florida, plant communities are known to recover quite quickly after a fire. Consequently, an eight month gap between fire suppression and the burn severity assessment is rather substantial and might have led to an underestimate of burn severity for the communities mapped within the Deep Fire. This suggests that dNBR may not be a good estimator of burn severity if a significant temporal gap exists between fire suppression and when the burn severity

assessment is conducted for communities whose species are well adapted to fire and demonstrate a propensity to recover quickly following fire.

Both the RGB-Reflectance and $G_{NDVI}PVI$ indices responded as expected and appear to be good predictors of post-fire community photosynthetic capacity reduction and burn severity (**Figure 5**). RGB-Reflectance increased between 2009 and 2010 in response to a significant decrease in palisade mesophyll absorption of the blue and red wavelength while $G_{NDVI}PVI$ decreased as a result of a significant reduction in live biomass and reflectance in the green wavelength (**Figure 4**). Overall, $\Delta G_{NDVI}PVI(\%)$ showed the highest correlation to dNBR and, as such, could be used, after further evaluation, to act a surrogate to dNBR when the available imagery lacks a mid-infrared band.

References:

- Escuin., E., R. Navarro, and P. Fernandez. 2008. Fire severity assessment by using NBR (Normalized Burned Ratio) and NDVI (Normalized Difference Vegetation Index) derived from LANDSAT TM/ETM images. *International Journal of Remote Sensing*. 29(4):1053-1073.
- Gitelson, A.C., Y.J. Kaufman, M.N. Merzlyak. 1996. Use of a green channel in remote sensing of global vegetation from EOS-MODIS. *Remote Sensing of Environment* 58:289-298.
- Key C.H, and N.C. Benson. 2006. Landscape assessment: sampling and analysis methods. In D.C. Lutes, R.E. Keane, J.F. Caratti, C.H. Key, N.C. Benson, S. Sutherland, L.J. Gangi (Eds.). FIREMON: Fire Effects Monitoring and Inventory System. General Technical Report RMRS-GTR-164-CD. USDA Forest Service, Rocky Mountain Research Station, Fort Collins, CO. http://frames.nbii.gov/projects/firemon/FIREMON_LandscapeAssessment.pdf
- Motohka, T. K. N. Nasahara, H. Oguma, and s. Tsuchida. 2010. Application of green-red vegetation index for remote sensing of vegetation phenology. *Remote Sensing* 2: 2369-2387; DOI: 10.3390/rs2102369.
- Slocum, M.G., W.J. Platt, B. Beckage, B. Panko, and J.B. Lushine. 2007. Decoupling natural and anthropogenic fire regimes: a case study in Everglades National Park, Florida. *Natural Areas Journal* 27: 41-55.
- StatSoft Inc. 2005. *Statistica for Windows*. StatSoft Inc., Tulsa, OK, USA.
- Snyder, J.R. 1991. Fire regimes in subtropical South Florida. In 'Proceedings of the Tall Timbers Fire Ecology Conference No. 17 – High intensity fire in wildlands: management challenges and options. 18–21 May 1989. pp. 303–319. (Tall Timbers Research Station: Tallahassee, FL)
- The Nature Conservancy and Environmental Systems Research Institute. 1994. NBS/NPS Vegetation Mapping Program: Standardized National Vegetation Classification System. 112 pp. Report to the United States Department of Interior United States Geological Survey and National Park Service.
- Wade D, J. Ewel, and R. Hofstetter. 1980. Fire in south Florida ecosystems. USDA Forest Service, Southeastern Forest Experiment Station General Technical Report SE-17. (Asheville, NC)
- Warren, G. and G. Metternicht. 2005. Agricultural applications of high-resolution digital multispectral imagery: evaluating within-field spatial variability of canola (*Brassica napus*) in Western Australia. *Photogrammetric Engineering & Remote Sensing* 71(5): 595-602.
- Watts, A.C., L.N. Kobziar, and J.R. Snyder. 2012. Fire reinforces structure of pondcypress (*Taxodium distichum* var. *imbricarium*) domes in a wetland landscape. *Wetlands* 32(3): 439-448 DOI: 10.1007/s13157-012-0277-9.
- Welch, R., M. Madden, and R.F. Doren. 1999. Mapping the Everglades. *Photogrammetric Engineering and Remote Sensing*. 65(2): 163-170.

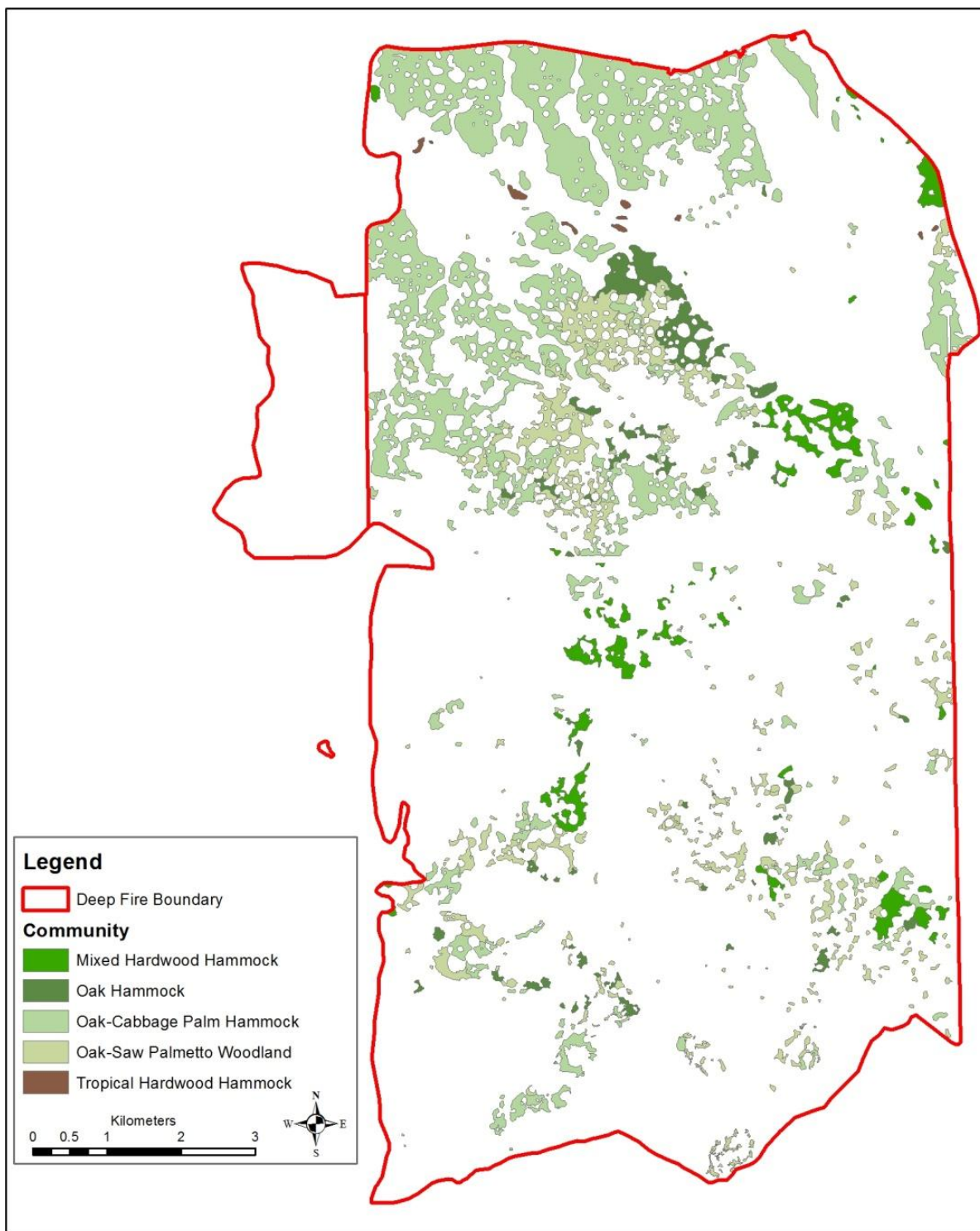


Figure 2: Thematic map of oak-dominated forest and hammocks within the Deep Fire.

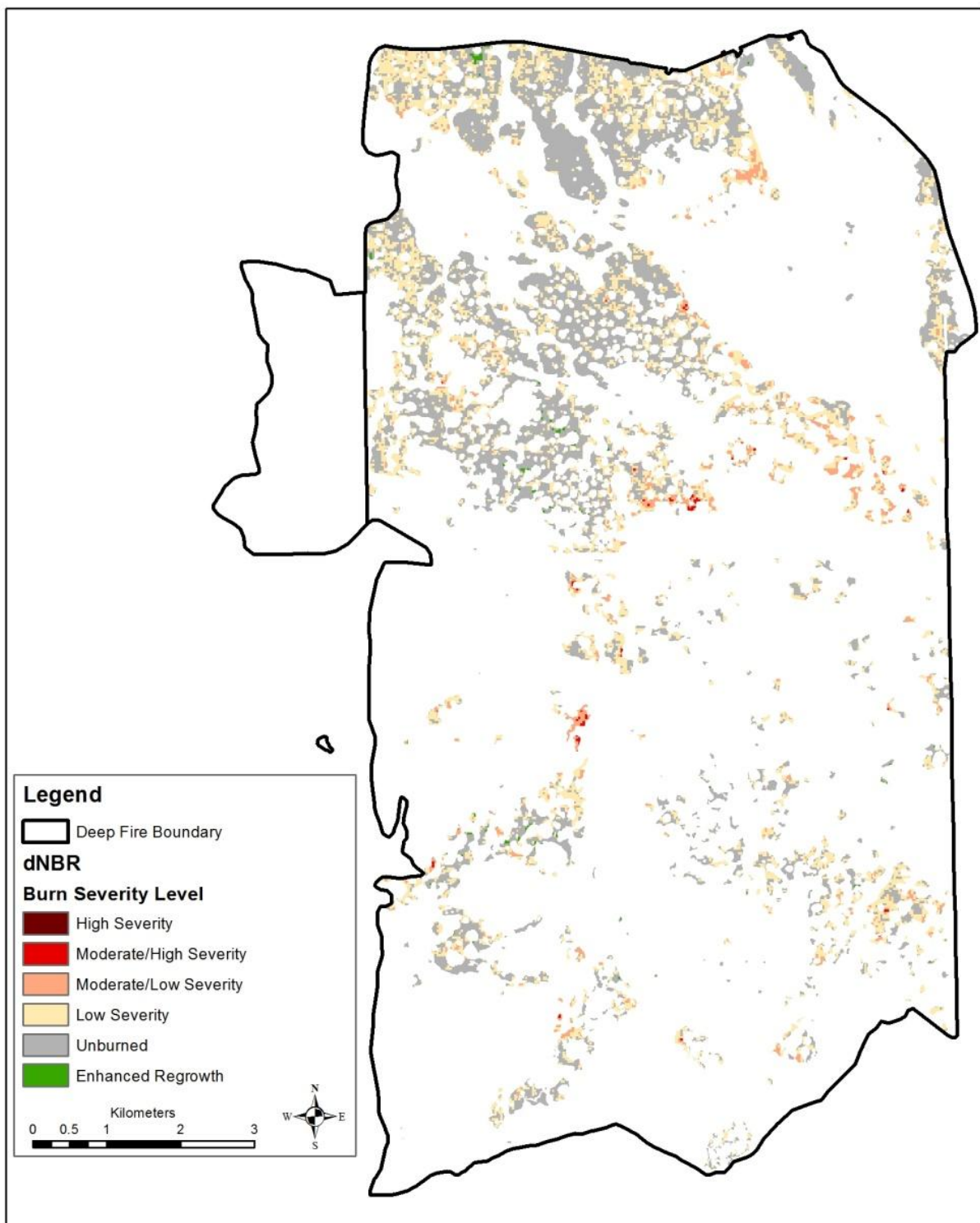


Figure 3: Burn severity (dNBR) map of oak-dominated forests and hammocks within the Deep Fire (2009).

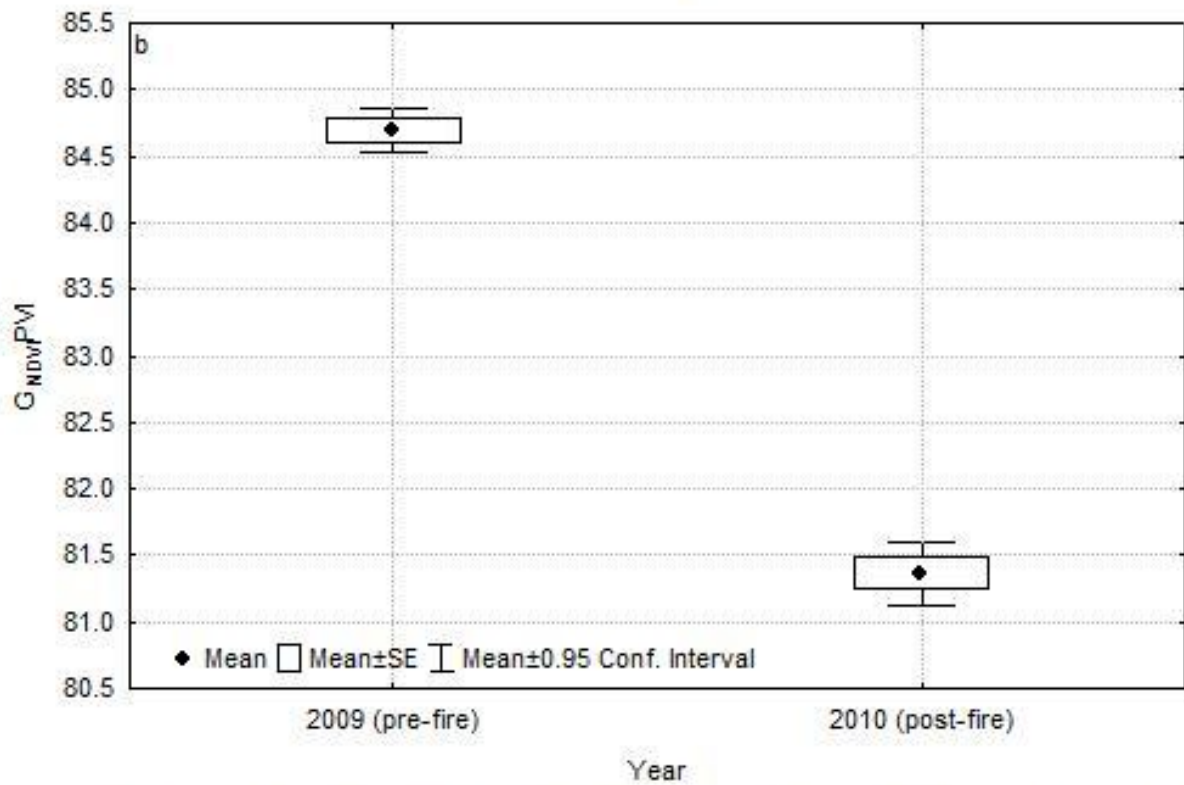
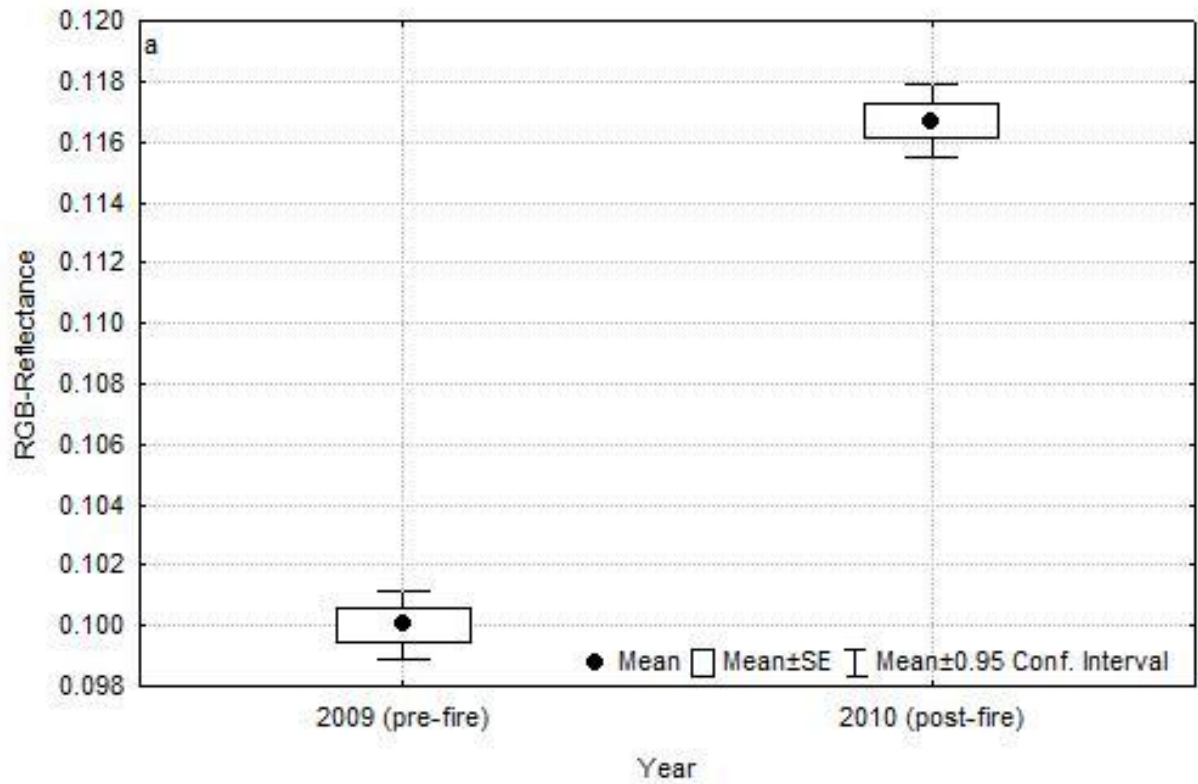


Figure 4: Pre- and post fire differences in (a) RGB-Reflectance and (b) $G_{NDVI} PVI$ for the oak-dominated forest and hammocks within the Deep Fire (2009).

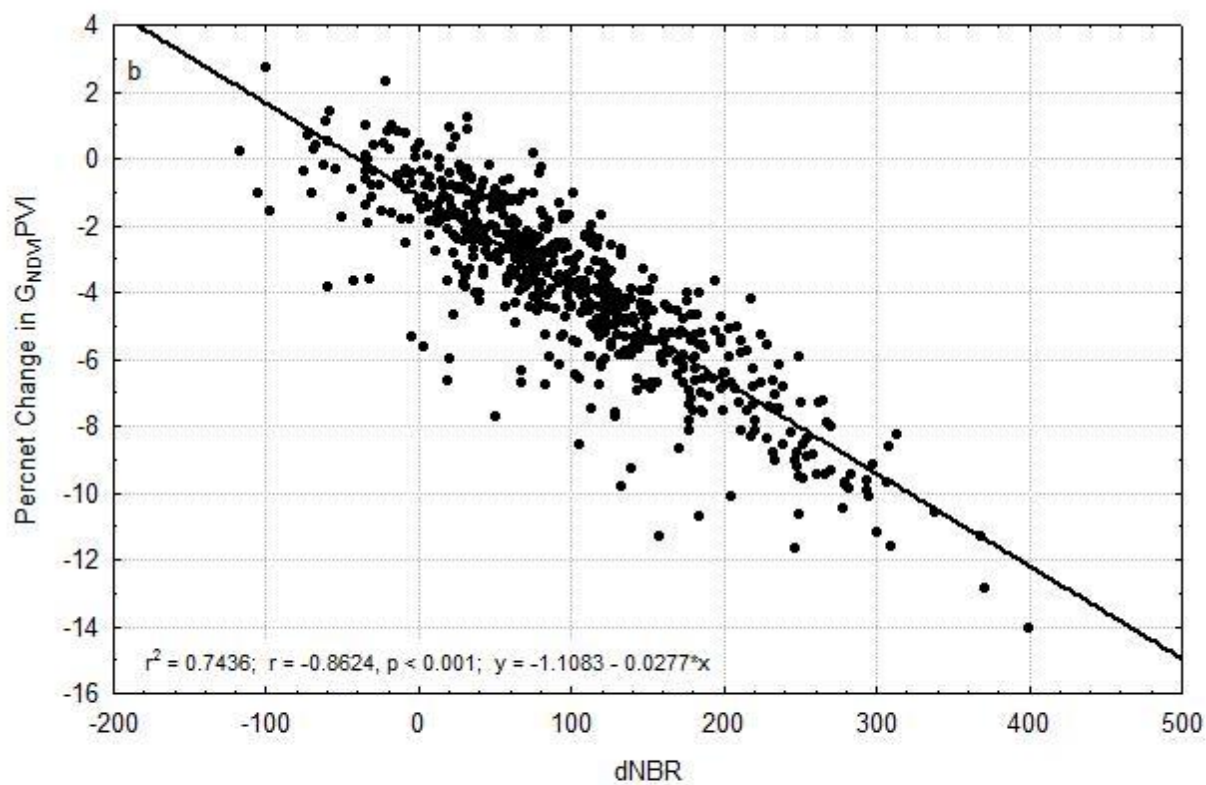
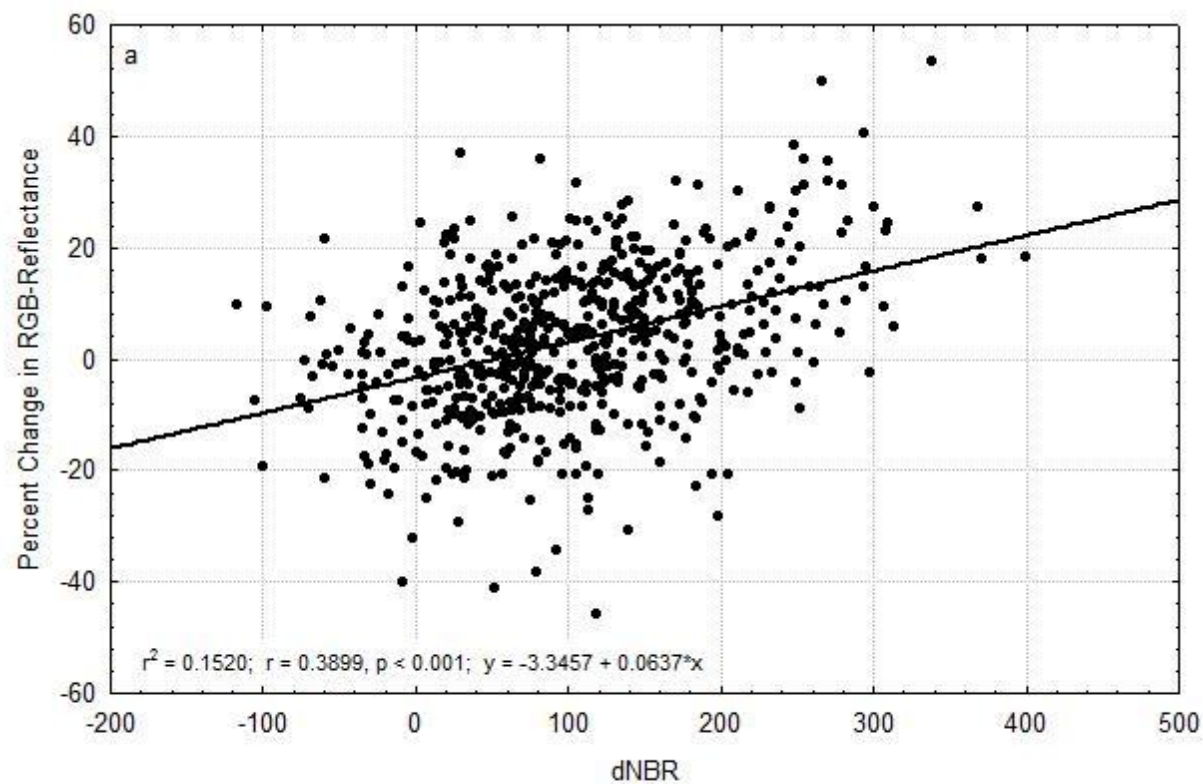


Figure 5: Correlation between dNBR and (a) percent change in RGB-Reflectance and (b) percent change in G_{NDVI}^{PVI} .